Onedimensional transport of warm electrons in In0.53Ga0.47As quantum well wires at low temperatures

D. Chattopadhyay and P. K. Ghosh

Citation: Journal of Applied Physics **75**, 7400 (1994); doi: 10.1063/1.356655
View online: http://dx.doi.org/10.1063/1.356655
View Table of Contents: http://scitation.aip.org/content/aip/journal/jap/75/11?ver=pdfcov
Published by the AIP Publishing

One-dimensional transport of warm electrons in $In_{0.53}Ga_{0.47}As$ quantum well wires at low temperatures

D. Chattopadhyay and P. K. Ghosh
Institute of Radiophysics and Electronics, 92 Acharya Prafulla Chandra Road, Calcutta 700 009, India

(Received 20 September 1993; accepted for publication 31 January 1994)

The ohmic mobility μ_0 and the warm electron coefficient β of the electrons moving one-dimensionally in a quantum well wire (QWW) of $In_{0.53}Ga_{0.47}As$ are investigated for lattice temperatures in the range of 4–10 K. Deformation potential acoustic, piezoelectric, ionized-impurity, and alloy scatterings are included considering the nonequipartition of phonons. β values are calculated by two models: one using a heated Fermi–Dirac distribution function, and the other using a more general moment method. Momentum relaxation is found to be controlled predominantly by alloy scattering. μ_0 is larger for a QWW of greater cross section and decreases slowly with the increase of the lattice temperature. In both models used here, β is negative; its magnitude falls with increasing lattice temperature and is greater for larger cross sections of the QWW. However, $|\beta|$ is larger in the heated Fermi–Dirac distribution function model.

I. INTRODUCTION

The fabrication, physics, and application of quantum well wires (QWW) formed between the closely spaced heterojunction interfaces of two different semiconductors have been receiving increasing attention in recent years.[1–8] In such structures, the electron gas is quantized in two transverse directions and executes one-dimensional (1D) motion in the longitudinal direction. Electronic transport in 1D systems is interesting because the density of states and the scattering rates are different from those of two-dimensional (2D) structures and of the bulk.[2] In this article, we study a 1D electronic transport in $In_{0.53}Ga_{0.47}As$ QWW in the warm-electron region where nonohmic behavior begins to appear. The low effective mass in (In,Ga)As offers a high mobility, promising for devices. Also, (In,Ga)As devices can be integrated with optoelectronic components in communication systems.

We calculate the ohmic mobility μ_0 and the warm-electron coefficient β for a degenerate electron distribution for lattice temperatures in the range of 4–10 K which is important for practical applications.[9] Carrier scatterings via ionized impurities, acoustic phonons through deformation potential and piezoelectric couplings, and alloy disorder are considered. We assume a heated Fermi–Dirac distribution in Sec. II for a basic understanding of the warm-electron behavior. In Sec. III we remove this assumption and use a more general moment method. In Sec. IV, we study the dependence of μ_0 and β on the cross section of the QWW and discuss the results in terms of the scattering processes and the assumed models.

II. ELECTRON TEMPERATURE MODEL

We consider a square cross section of a QWW with side lengths $L=8$ and 12 nm and a typical 1D carrier concentration $n_{1D}=9.6\times10^7$ m^{-1}. The lowest and the next higher subbands are found to be separated by an energy one order of magnitude greater than the average electron energy here. The population of the higher subbands can thus be neglected, and the electrons can be assumed to be confined to the lowest subband.

In this section, we adopt the popular electron temperature model,[10] and thus take the symmetric part of the distribution function $f_0(E)$ to be a heated Fermi–Dirac function characterized by an electron temperature T_e. Here, E is the electron energy for motion in the longitudinal direction, i.e., $E=\hbar^2k_z^2/(2m^*)$ where $\hbar$ is Planck's constant divided by 2π, k_z is the 1D wave vector in the longitudinal z direction, and m^* is the electron effective mass.

In a rectangular Cartesian frame, we take x and y directions along the two adjacent sides of the cross section of the QWW and the z direction along the axis of the wire to which an electric field $\mathscr{E}$ is applied. The momentum relaxation times τ_{ac} and τ_{pz} for deformation potential acoustic and piezoelectric scattering, respectively, and the energy loss rates $\langle dE/dT\rangle_{ac}$ and $\langle dE/dT\rangle_{pz}$ for these two scattering processes are found from the square of the matrix element for the 1D system.[11,12] In the energy loss rates, the terms up to the linear in (T_e-T_l) are kept, T_l being the lattice temperature, because these are the only important terms in the warm-electron regime.[13] The nonequipartition of the acoustic phonons is considered in the calculations done numerically.

The momentum relaxation time τ_{im} for background impurity scattering was derived by Lee and Vassell.[2] We use their expression here for a typical background impurity concentration of 5×10^{21} m^{-3}. The effect of remote impurities is small for a thick undoped spacer in modulation doped structures, and so it is not considered here. The momentum relaxation time for alloy disorder scattering τ_{al}, as given by Basu *et al.*,[14] is used.

The electron mobility is given by

$$\mu=\frac{2e}{\pi\hbar n_{1D}}\left(\frac{2}{m^*}\right)^{1/2}\int_0^\infty E^{1/2}\tau\left(-\frac{\partial f_0}{\partial E}\right)dE, \tag{1}$$

where e is the electronic charge and $\tau^{-1}=\tau_{ac}^{-1}+\tau_{pz}^{-1}+\tau_{im}^{-1}+\tau_{al}^{-1}$.

 0021-8979/94/75(11)/7400/4/$6.00

For an applied electric field $\mathscr{E}$, the warm-electron mobility is

$$\mu=\mu_0(1+\beta\mathscr{E}^2), \tag{2}$$

the higher order terms in $\mathscr{E}$ being insignificant. We expand μ in a Taylor series in (T_e-T_l) and keep only the first order terms in (T_e-T_l); we obtain

$$\mu=\mu_0+(T_e-T_l)\left.\frac{d\mu}{dT_e}\right|_{T_e=T_l}. \tag{3}$$

The balance of energy relationship is

$$e\mu_0\mathscr{E}^2=-\left\langle\frac{dE}{dt}\right\rangle_{ac}-\left\langle\frac{dE}{dt}\right\rangle_{pz}=(T_e-T_l)s(T_l), \tag{4}$$

where the function $s(T_l)$ is obtained numerically from the energy loss rates.[12]

From Eqs. (2), (3), and (4) the warm-electron coefficient β is found to be

$$\beta=\frac{e}{s(T_l)}\left.\frac{d\mu}{dT_e}\right|_{T_e=T_l}, \tag{5}$$

with $d\mu/dT_e|_{T_e=T_l}$ being obtained from Eq. (1).

Although the electron temperature model is simple and gives insight into carrier kinetics, it is actually established for very strong electron-electron scattering. When strong carrier-carrier scattering does not prevail, as in the case of 1D transport, the distribution function deviates from the heated Fermi–Dirac form.[15] We include this deviation in Sec. III. We find that, although the electron temperature model gives the correct nature of the variation of β with system parameters, it predicts values too large for $|\beta|$ (shown later in Fig. 5).

III. GENERAL MODEL

In general, one can express $f_0(E)$ as a power series in $\mathscr{E}$ and retain only terms of order $\mathscr{E}^2$ in the warm-electron range.[16] We thus write

$$f_0(E)=C|1+\mathscr{E}^2\phi(E)|f_L(E), \tag{6}$$

where $f_L(E)$ is the Fermi–Dirac function at the lattice temperature T_l and C is a constant determined by the requirement that the sum of f_0 over the available states yields the carrier density. The Boltzmann equation gives

$$\frac{e^2}{m^*}\tau\frac{\partial f_L}{\partial E}+\left(\frac{2e^2}{m^*}E\right)\frac{\partial}{\partial E}\left(\tau\frac{\partial f_L}{\partial E}\right)+\left(\frac{\partial\phi f_L}{\partial t}\right)_{\text{coll}}=0, \tag{7}$$

where $(\partial f_0/\partial t)_{\text{coll}}$ is calculated for deformation-potential acoustic and piezoelectric scatterings from the relevant matrix elements, as was discussed in Sec. II.

We expand $\phi(E)$ as a power series in E:

$$\phi(E)=\sum_{r=1}^{p}a_rE^r, \tag{8}$$

and determine the coefficients a_r by the method of moments.[16] In this method, Eq. (7) is multiplied by E^rdE and the result is integrated for all values of E. The coefficient a_r is found by solving p number of equations obtained by varying r from 1 through p. The mobility is calculated from Eq. (1) and β from Eq. (2). Convergent values are found with p between 9 and 12.

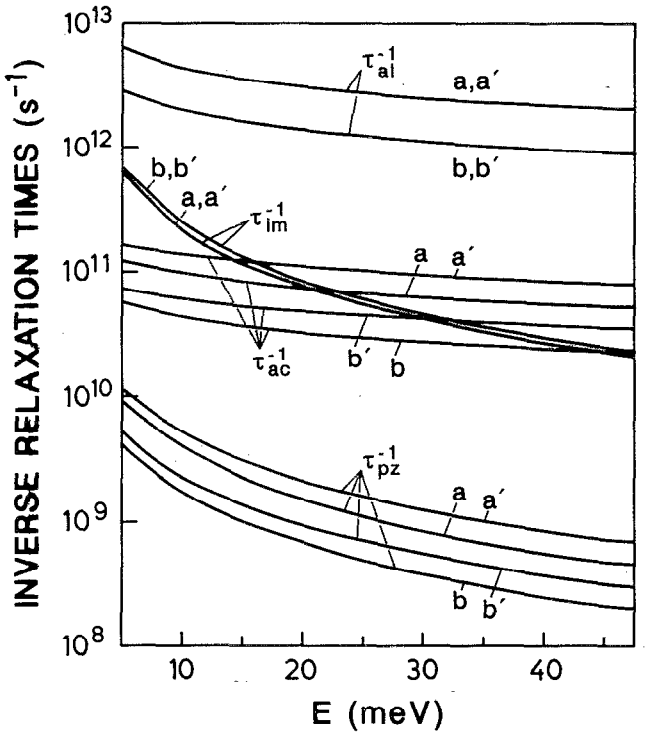

FIG. 1. Plot of the inverse relaxation times τ_{al}^{-1}, τ_{im}^{-1}, τ_{ac}^{-1}, and τ_{pz}^{-1} vs the electron energy E. Curves a and b are for a lattice temperature of 6 K with $L=8$ and 12 nm, respectively. Curves a′ and b′ are for 10 K with $L=8$ and 12 nm, respectively.

IV. CALCULATED RESULTS AND CONCLUSIONS

The material parameters of (In,Ga)As given in Ref. 14 are used in the calculations. Figure 1 shows the plot of the inverse relaxation times for the different scattering mechanisms versus the electron energy E. The inverse relaxation times decrease with increasing E because the density of states in the QWW varies as $E^{-1/2}$. With a rise in the lattice temperature, the phonon occupation number increases, leading to an enhancement of deformation-potential acoustic and piezoelectric scattering rates. As the cross sectional area of the QWW increases, the phonon and the alloy disorder scattering rates decrease, but the impurity scattering rate increases slightly. The alloy scattering is found to dominate the momentum relaxation.

The dependence of μ_0 on the lattice temperature is displayed in Fig. 2. The mobility is found to decrease slightly with increasing temperature. With a rise in temperature, the electrons move to the high energy states. The fall of the density of states at high energies overrides the increase of the momentum relaxation time at such energies, causing the mo-

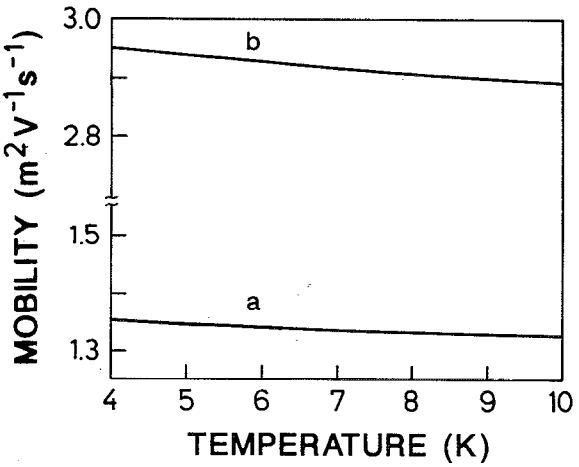

FIG. 2. Variation of the ohmic mobility μ_0 with lattice temperature. Curves a and b are for $L=8$ and 12 nm, respectively.

bility to decrease with an increase in temperature. The mobility increases with an increase of L because the alloy scattering rate controlling the mobility falls.

Figure 3 shows the variation of $(d\mu/dT_e)_{T_l}$ with lattice temperature. $(d\mu/dT_e)_{T_l}$ is negative, alloy scattering being important. As the temperature increases, $|(d\mu/dT_e)_{T_l}$ decreases since the density of states varies as $E^{-1/2}$. For a higher L, $(d\mu/dT_e)_{T_l}$ is more negative as the alloy scattering is then weaker. As the temperature increases, the phonon occupation number increases, leading to an increase of the energy loss rate. So, the function $s(T_l)$ increases with temperature, as is seen in Fig. 4. Deformation-potential acoustic scattering controls the energy loss rate, with piezoelectric scattering contributing 2 orders of magnitude less. As L increases, $s(T_l)$ is reduced, with phonon scattering being weaker.

The warm-electron coefficient β is negative here since $(d\mu dT_e)_{T_l}$ is negative. Figure 5 shows that $|\beta|$ decreases with an increase in the lattice temperature. The rise of $s(T_l)$ coupled with the fall of $|(d\mu/dT_e)_{T_l}|$ with temperature ac-

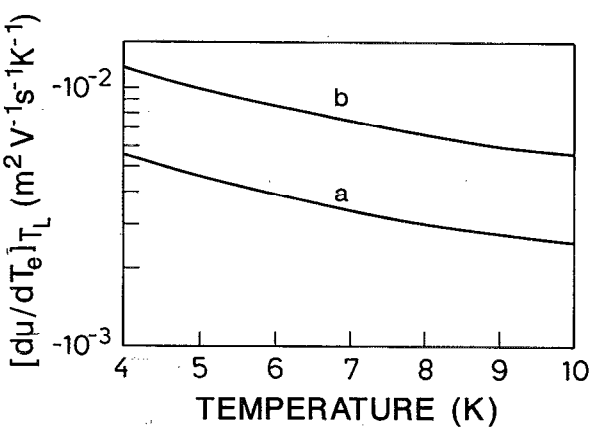

FIG. 3. Plot of $(d\mu/dT_e)_{T_l}$ with lattice temperature. Curves a and b have the same significance as in Fig. 2.

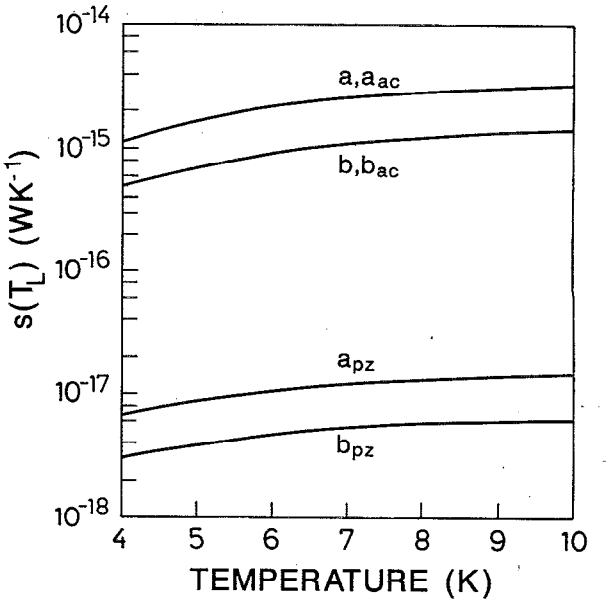

FIG. 4. Plot of $s(T_l)$ with lattice temperature. Curves a and b have the same meaning as in Fig. 2. Curves a_{ac} and a_{pz} show the contributions of deformation-potential acoustic and piezoelectric scattering to curve a. Curves b_{ac} and b_{pz} show the same contributions to curve b. Curves a_{ac}, a and b_{ac}, b are not separable in the scale of the plot.

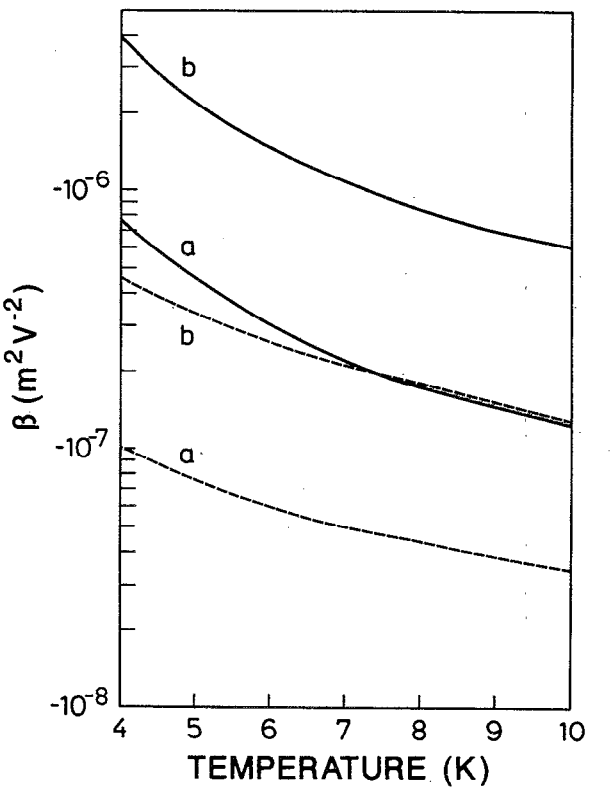

FIG. 5. Variation of the warm-electron coefficient with lattice temperature. Curves a and b have the same meaning as in Fig. 2. The solid curves give the values in the electron temperature model and the dashed curves give those in the general model.

counts for this behavior of β. For a greater cross sectional area of the QWW, β is more negative since $s(T_l)$ is lower and $|(d\mu/dT_e)_{T_l}|$ is higher for greater L. The sign of β is different from that for a GaAs QWW where alloy scattering is absent.[12]

Figure 5 also shows that, when the assumption of electron temperature is removed, the general behavior of β with regard to the lattice temperature and the width of the QWW remains the same. The dependence of β on the system parameters is thus correctly understood in terms of the heated Fermi–Dirac distribution. However, the values of $|\beta|$ obtained in the general model are smaller than those obtained in the electron temperature model. The warm-electron coefficient is, thus, sensitive to the form of the distribution function.

The warm-electron condition prevails for fields much less than $1/\sqrt{\beta}$. At an ambient temperature of 8 K, the effect is thus observed for fields of about 500 V m^{-1}. Experimental data on warm electron transport in a QWW have not yet appeared, though β has been measured for a 2D electron gas in GaAs/(Al,Ga)As heterojunction.[17] Similar measurements in a (In,Ga)As QWW are required for a comparison with the calculations reported here.

ACKNOWLEDGMENT

One of us (D.C.) expresses his gratitude to Dr. H. J. Queisser for hospitality at the Max-Planck-Institut für Festkörperforschung, Stuttgart, where a part of the work was done. P.K.G. acknowledges the financial support of the Council of Scientific and Industrial Research (CSIR), India.

[1] P. Petroff, A. Gossard, R. Logan, and W. Wiegmann, Appl. Phys. Lett. **41**, 635 (1982).
[2] J. Lee and M. O. Vassell, J. Phys. C **17**, 2525 (1984).
[3] D. Chattopadhyay and A. Bhattacharyya, Phys. Rev. B **37**, 7105 (1988).
[4] A. Kabasi, D. Chattopadhyay, and C. K. Sarkar, Semicond. Sci. Technol. **3**, 1025 (1988).
[5] M. Tsuchiya, J. M. Gains, R. H. Yan, R. J. Sines, P. O. Holtz, L. A. Coldren, and P. M. Petroff, J. Vac. Sci. Technol. B **7**, 315 (1989).
[6] J. Sone, Semicond. Sci. Technol. B **7**, 210 (1992).
[7] J. S. Weiner, J. M. Calleja, A. Pinczak, A. Schmeller, B. S. Dennis, A. R. Goni, L. N. Pfeiffer, and K. W. West, Appl. Phys. Lett. **63**, 237 (1993).
[8] T. Nishida, H. Sugiura, M. Notomi, and T. Tamamura, J. Cryst. Growth **132**, 91 (1993).
[9] S. Datta and M. J. Mclennan, Rep. Prog. Phys. **53**, 1003 (1990).
[10] See, for example, K. Hess, in *Physics of Non-linear Transport in Semiconductors*, edited by D. K. Ferry, J. R. Barker, and C. Jacoboni (Plenum, New York, 1980), pp. 1–42.
[11] P. J. Price, Ann. Phys. (New York) **133**, 217 (1981).
[12] A. Kabasi and D. Chattopadhyay, Solid State Commun. **75**, 71 (1990).
[13] K. Seeger, *Semiconductor Physics* (Springer, Wien, 1973), Chaps. 4 and 6.
[14] P. P. Basu, D. Chattopadhyay, and P. C. Rakshit, Phys. Rev. B **46**, 13254 (1992).
[15] J. Yamashita and M. Watanabe, Progr. Theoret. Phys. **12**, 443 (1954).
[16] E. M. Conwell, *High Field Transport in Semiconductors*, in Solid State Physics, Suppl. 9, edited by F. Seitz, D. Turnbull, and H. Ehrenreich (Academic, New York, 1967), pp. 269–270.
[17] K. Tsubaki, A. Sugimura, and K. Kumabe, Appl. Phys. Lett. **46**, 764 (1985).